J. exp. Biol. (1978), 76, 85–104
With 9 figures
Printed in Great Britain

A QUANTITATIVE ANALYSIS OF FLAGELLAR MOVEMENT IN ECHINODERM SPERMATOZOA

BY YUKIO HIRAMOTO

Biological Laboratory, Tokyo Institute of Technology, Meguro-ku, Tokyo 152, Japan

AND SHOJI A. BABA

Zoological Institute, University of Tokyo, Hongo, Tokyo 113, Japan

(*Received 20 December 1977*)

SUMMARY

Computerized analyses were performed on the movement of spermatozoa recorded with a high-speed camera. These provide evidence for active bending waves over the entire length of the flagellum and a single equation for waves in all cases examined. In the equation, the angular direction of the flagellum at any distance from the base is expressed by a sine function of time plus a constant, and thus flagellar waves are 'sine-generated'. To explain the waves a model was proposed in which the active force required to generate sliding between peripheral microtubules is propagated along and around the flagellar axoneme.

INTRODUCTION

An accurate description of the bending wave of flagella is important in understanding the mechanism of flagellar movement, but detailed analyses have rarely been carried out. In the present study we have photographed the movement of sperm flagella at the limit of resolution of the light microscope, analysed the waveforms in various environments with a computer, and have derived a single equation which adequately describes the waveforms in all cases examined. In this equation, the angular direction of the flagellar shaft is expressed as a sine function of time plus a constant, that is, the wave is regarded as a sine-generated wave which is an approximation of the wave of minimum energy expenditure (cf. Silvester & Holwill, 1972). It will be shown that the sine-generated wave can be explained as a result of force generation for sliding at sites between neighbouring peripheral microtubules in flagellar axonemes on the basis of a model in which the activation of the force generation propagates along and around the axoneme.

MATERIALS AND METHODS

Spermatozoa

Spermatozoa were obtained from the gonad dissected from the starfish, *Asterias amurensis*, and from the sea urchin, *Hemicentrotus pulcherrimus*, by injection of 0·54 M-KCl into the body cavity. The sperm sample was observed with a phase-contrast microscope after dilution with filtered sea water. In the case of the starfish spermatozoa, the sea water contained 1 mM-L-histidine, which enhanced the motility of the sperm (Fujii, Utida & Mizuno, 1955), and sometimes polyvinylpyrrolidone (< 4%), which increased the viscosity of the medium (see Table 2; cf. Baba & Hiramoto, 1970*b*).

Recording

The movement of spermatozoa was recorded with a high-speed camera (Himac 16HS, Hitachi) as described in previous reports (Baba & Hiramoto, 1970*a*, *b*). The filming rate of the camera was set appropriately by controlling the driving voltage and determined by counting time signals simultaneously recorded on the margin of film; the framing rate was usually about 500 p.p.s. though it was reduced when spermatozoa were swimming slowly in media of increased viscosity. The ratio of exposure time to the interval between frames was adjusted to be about 1/25 by using a slit of the proper width in the illumination system (cf. Baba & Hiramoto, 1970*a*, *b*) so that the exposure time was always short enough (< 100 μs at 500 p.p.s.) to record clearly the relatively rapid movement of sperm tails. The phase-contrast objective lenses used were 40× (Nikon BM 40/0·65) and 100× (Nikon BM 100/1·25 and Plan BM 100/1·30 oil immersion) objectives; the results shown in the present paper were obtained using the 100× objectives, unless otherwise stated.

Recordings were made of spermatozoa swimming close (*ca.* 2 μm) to and far (*ca.* 300 μm) from the coverslip surface in a trough 1 mm in depth. For spermatozoa within 2 μm of the surface, it was not difficult to focus the entire image accurately, because the cells were swimming along circular paths with the beat plane of their tails parallel to the coverslip. For spermatozoa swimming far from the coverslip, the 40× objective was used and its plane of focus was set about 300 μm below the surface; spermatozoa which swam at this level were recorded. Recordings were also made of spermatozoa attached by their heads to the jelly layer of eggs or to the vertical cut edge of a thin layer of agar gel (0·5%). Because the spermatozoa adhered firmly to the cut edge of agar gel, it was not difficult to find a spermatozoon with a beat plane either parallel to or perpendicular to the plane of focus.

Analysis

All cinematographs taken were projected at a normal (16 p.p.s.) or reduced speed onto a screen, and routine measurements were made by tracing the swimming track and waveform of spermatozoa. Sharply focused sequences were selected for a detailed frame-by-frame analysis. The time t of frames was determined from the framing rate of the sequence. On a Cartesian system with the X-axis approximately parallel to the wave axis, the coordinates of points on the head and tail images were obtained from enlarged prints on a shadowgraph (Nikon, Model 6C) or directly

from the projection of negatives on a film motion analyser (Osawa, Model F-107); the final magnification was 25000 times on the shadowgraph and 1000–5000 times on the motion analyser. The head centre $\mathbf{Q}_H(t)$ was recorded, and the apex of the head and the flagellar base were used to define the angular direction $\phi_H(t)$ of the head (with respect to the X-axis of coordinates). Points were obtained at intervals of 1–2 μm along the flagellum, giving about 50 points in all from the image of a single spermatozoon. In most cases these measurements were repeated three times for each image (see Fig. 3).

As the first step in analysing the flagellar waveform, all combinations of three neighbouring points along the flagellum were used to define circles of known radius and hence curvature. The calculated curvature was assumed to represent that of the flagellar shaft at the middle of the three points and, in the case of both ends of the flagellum, at the terminal as well as the middle point. Then, every segment between two neighbouring points was approximated by a single circular arc, the curvature of which was given by averaging the curvatures determined above at the two points. The curvature $\gamma(s, t)$ was thus given as a step function of distance s measured from the base along the flagellum (see Fig. 4). After this procedure, points were taken at regular intervals of Δs (usually 0·5 μm) along the approximate waveform defined by a connected series of the circular arcs. The coordinates $\mathbf{Q}(s, t)$ of the points were calculated, using each set of data obtained by the repeated measurements referred to previously, and were averaged for use in reproducing waveforms (see Fig. 3) and in further analyses.

The angular direction of the flagellar shaft at a point $\mathbf{Q}(s, t)$ was approximated by that of the line connecting two points, proximal and distal to the point by Δs, i.e. $\mathbf{Q}(s+\Delta s, t)$ and $\mathbf{Q}(s-\Delta s, t)$, and was computed at intervals of Δs as $\phi^x(s, t)$ with respect to the X-axis of coordinates and as $\phi^h(s, t)$ with respect to the head axis. The angles ϕ^x and ϕ^h were fitted using equations of the form:

$$\phi(s, t) = \phi_a(s) \cos\{S_\phi(s) - \omega(s)\, t\} + \phi_b(s), \qquad (1)$$

with fixed s and varying t. The fitting was performed by the method of least squares for non-linear functions (Powell, 1965; cf. Bevington, 1969), using a program written by Dr Y. Oyanagi filed in the program library (C7/TCPOW1) of the Computer Centre of the University of Tokyo. The parameters ϕ_a, S_ϕ and ω are the amplitude, phase angle and angular velocity, respectively, of the cosine component of ϕ, while ϕ_b is a constant which represents mean direction of the flagellum at distance s during one cycle. In the case of ϕ^x, ϕ_b may vary when the cell progresses, and therefore it is not always independent of time t. In the present study ϕ_b was, however, assumed to remain constant during one cycle and was analysed only as a function of s. Otherwise, equation (1) was appropriate for ϕ^x as well as ϕ^h; the suffixes x and h may be omitted when similar results were obtained for both ϕ^x and ϕ^h, or when it is not necessary to refer to the reference line of the shaft angle.

The velocity $\mathbf{V}(s, t)$ of a point $\mathbf{Q}(s, t)$ on the flagellum and the velocity $\mathbf{V}_H(t)$ of the head centre $\mathbf{Q}_H(t)$ were calculated from the displacement of the points between two frames preceding and next to the frame of time t divided by twice the interval, Δt, of the successive frames as follows,

$$\mathbf{V}(s, t) = \{\mathbf{Q}(s, t+\Delta t) - \mathbf{Q}(s, t-\Delta t)\}/(2\Delta t),$$

and

$$\mathbf{V}_H(t) = \{\mathbf{Q}_H(t+\Delta t) - \mathbf{Q}_H(t-\Delta t)\}/(2\Delta t). \quad (2)$$

The resistance $\mathbf{F}_H(t)$ for movement of the head was calculated by the equation,

$$\mathbf{F}_H = C_H a \mathbf{V}_H, \quad (3)$$

where a is the radius of the head. In this equation C_H is a resistance coefficient, which is given by

$$C_H = 6\pi\eta \Big/ \left\{1 - \frac{9}{16}\left(\frac{a}{h}\right) + \frac{1}{8}\left(\frac{a}{h}\right)^3 - \frac{45}{256}\left(\frac{a}{h}\right)^4 + \ldots\right\} \quad \text{(cf. Happel \& Brenner, 1965)}, \quad (4)$$

where η is the viscosity of the medium and h is the distance of the head centre from the coverslip surface. The resistance $\Delta\mathbf{F}(s, t)$, which acts on a minute segment of length Δs of the flagellum, is a vector sum of the component forces $\Delta\mathbf{F}_N$ and $\Delta\mathbf{F}_L$ normal to and along the flagellar axis. $\Delta\mathbf{F}_N$ and $\Delta\mathbf{F}_L$ were calculated from the following equations,

$$\Delta\mathbf{F}_N = C_N \mathbf{V}_N \Delta s,$$

and

$$\Delta\mathbf{F}_L = C_L \mathbf{V}_L \Delta s \quad \text{(cf. Gray \& Hancock, 1955)}, \quad (5)$$

where C_N and C_L are coefficients of resistance for movement of the segment normal to and along the axis respectively while $\mathbf{V}_N$ and $\mathbf{V}_L$ are the component velocities in the two directions. C_N and C_L are given by the equations,

$$C_N = 4\pi\eta/\ln(2h/r),$$

and

$$C_L = 2\pi\eta/\ln(2h/r) \quad \text{(Katz \& Blake, 1975)}, \quad (6)$$

when the distance h of the flagellum from the coverslip surface is comparable with the radius r of the flagellum, and when h is much larger than r they are given by

$$C_N = 4\pi\eta/\{\ln(2q/r) + 0{\cdot}5\},$$

and

$$C_L = 2\pi\eta/\ln(2q/r) \quad \text{(Lighthill, 1976)} \quad (7)$$

with the characteristic length $q = 0{\cdot}09\Lambda$ (where Λ is wavelength measured along the flagellum). In the intermediate range of h (e.g. $h = 3{\cdot}0\ \mu$m, see Table 1), values for C_N and C_L were corrected by exact equations given by Takaishi (1958) for straight circular cylinders of flagellar dimensions. Table 1 shows C_H/C_L, C_N/C_L and C_L/η from the appropriate equations for various values of h.

The moments $\Delta\mathbf{M}(s', s, t)$ and $\mathbf{M}_H(s, t)$ about a point $\mathbf{Q}(s, t)$ due to $\Delta\mathbf{F}(s', t)$ and $\mathbf{F}_H(t)$, respectively, were calculated from the equations,

$$\Delta\mathbf{M}(s', s, t) = \Delta\mathbf{F}(s', t) \times \{\mathbf{Q}(s', t) - \mathbf{Q}(s, t)\}, \quad (8)$$

and

$$\mathbf{M}_H(s, t) = \mathbf{F}_H(t) \times \{\mathbf{Q}_H(t) - \mathbf{Q}(s, t)\}. \quad (9)$$

The bending moment $m(s, t)$ about the point $\mathbf{Q}(s, t)$ due to viscous resistances is the sum of the moments due to the resistances acting on that part of the spermatozoon either distal to or proximal to the point. The moment due to the rotation of the head about its axis perpendicular to the beat plane by yawing of the spermatozoon was not

Table 1. *Theoretical values of resistance coefficients of swimming starfish spermatozoa*

h (μm)	1·2	1·5	2·0	3·0	∞
C_H/C_L	25	19	17	15	12
C_N/C_L	2·0	2·0	2·0	1·95	1·8
C_L/η	2·0	1·9	1·7	1·6	1·6

The values of C_H, C_N and C_L were obtained from equations (4), (6) and (7), where $a = 1{\cdot}2$ μm, $r = 0{\cdot}1$ μm and $\Lambda = 30$ μm were used. h is the distance of spermatozoa from the coverslip surface. η is the viscosity of the medium. See text for further details.

considered because it was calculated to be negligibly small (10^{-18} N m) from the rotation speed in the present study. For swimming spermatozoa the bending moment about a point $\mathbf{Q}(s, t)$ was determined by integrating $\Delta\mathbf{M}(s', s, t)$ along the flagellum with respect to s' from the base to that point and adding $\mathbf{M}_H(s, t)$. For spermatozoa adhering to agar it was determined by integrating $\Delta\mathbf{M}(s', s, t)$ with respect to s' from the distal end of the flagellum to the point because the force $\mathbf{F}_H$ acting on the head was unknown. The calculated viscous bending moment $m(s, t)$ was then used to give a convenient expression of the form,

$$m(s, t) = m_a(s) \cos \{S_m(s) - \omega t\} + m_b(s), \tag{10}$$

where the parameters m_a, S_m and m_b were determined by the least squares method.

Most calculations above were performed using programs written in Fortran (JIS 7000) at the Computer Centre (HITAC 8800/8700 System) of the University of Tokyo.

RESULTS

Movement of spermatozoa

Fig. 1 illustrates starfish spermatozoa in normal sea water when swimming and when adhering to agar gel; Fig. 2 illustrates spermatozoa in sea water of increased viscosity. The entire length of a spermatozoon is in focus when viewed in the direction perpendicular to the beat plane (Figs. 1*a*, *b*, 2*a*, *b*). This observation indicates that the spermatozoa execute planar flagellar beats; in Figs. 1 and 2 simplified planar beat patterns are shown as superimposed waveforms (*c* and *d*). When spermatozoa are viewed in the direction parallel to the beat plane, the limited depth of focus of the microscope used produces an effect of optical sectioning, giving images of flagella which appear as the straight dashed lines seen in Fig. 1(*e*). This straightness of the dashed-line image indicates that the flagellar beat of sperm tails is planar irrespective of whether the beat plane is parallel to or perpendicular to the coverslip surface.

Table 2 shows the characteristic features of the movement of starfish and sea-urchin spermatozoa. Close to a coverslip spermatozoa swam along circular paths more frequently in the clockwise direction than the anticlockwise. Increasing the viscosity of the medium reduced both the speed and the beat frequency while the ratio of the two remained fairly constant. At about 300 μm from the coverslip, spermatozoa swam along spiral paths; the sense of the spirals was judged to be left-handed from the appearance of the image of the head, which moved repeatedly in and out of focus as the cells progressed. The speeds of their propulsion along the spiral paths calculated by a geometrical equation of spirals (cf. Gray, 1955) were higher than the

Table 2. *Characteristics of movement of spermatozoa*

Sperm (No. of spermatozoa)	Viscosity η (cP.)	Beat frequency f (Hz)	Swimming path (Sense)	Pitch (μm)	Diameter (μm)	Turn rate (Hz)	Speed of propulsion V (μm/s)	Speed of propulsion v (μm/beat)
Asterias								
Swimming 300 μm below a coverslip			Spirals					
(4)	1	43·3 ± 4·8	(Left-handed)	84 ± 4	24·8 ± 5·4	2·3 ± 0·3	259 ± 8	6·0 ± 0·7
Swimming close to a coverslip			Circles					
(15)	1	41·9 ± 3·1	(C-8; A-7)	—	139 ± 94	0·6 ± 0·3	203 ± 35	4·9 ± 0·7
(10)	11	2·1 ± 0·6	(C-5; A-2; S-3)	—	—	—	9·5 ± 2·5	4·6 ± 0·8
(3)	23	1·3 ± 0·9	(S-1)	—	—	—	6·0 ± 4·8	4·6 ± 0·4
Adhering by the head to agar gel								
(7)	1	32·3 ± 6·5						
(1)	11	4·0						
Hemicentrotus								
Swimming 300 μm below a coverslip			Spirals					
(12)	1	45·8 ± 4·6	(Left-handed)	34 ± 8	12·5 ± 1·9	4·8 ± 0·8	243 ± 15	5·4 ± 0·8
Swimming close to a coverslip			Circles					
(7)	1	42·9 ± 2·1	(C-7)	—	33·4 ± 6·8	1·7 ± 0·4	167 ± 13	3·9 ± 0·2

Mean ± S.D. Temperature: 20 ~ 23 °C.
C, Clockwise; A, anticlockwise; S, straight. For example, C-7 means that 7 spermatozoa recorded swim in circles in the clockwise direction.
$v = V/f$.

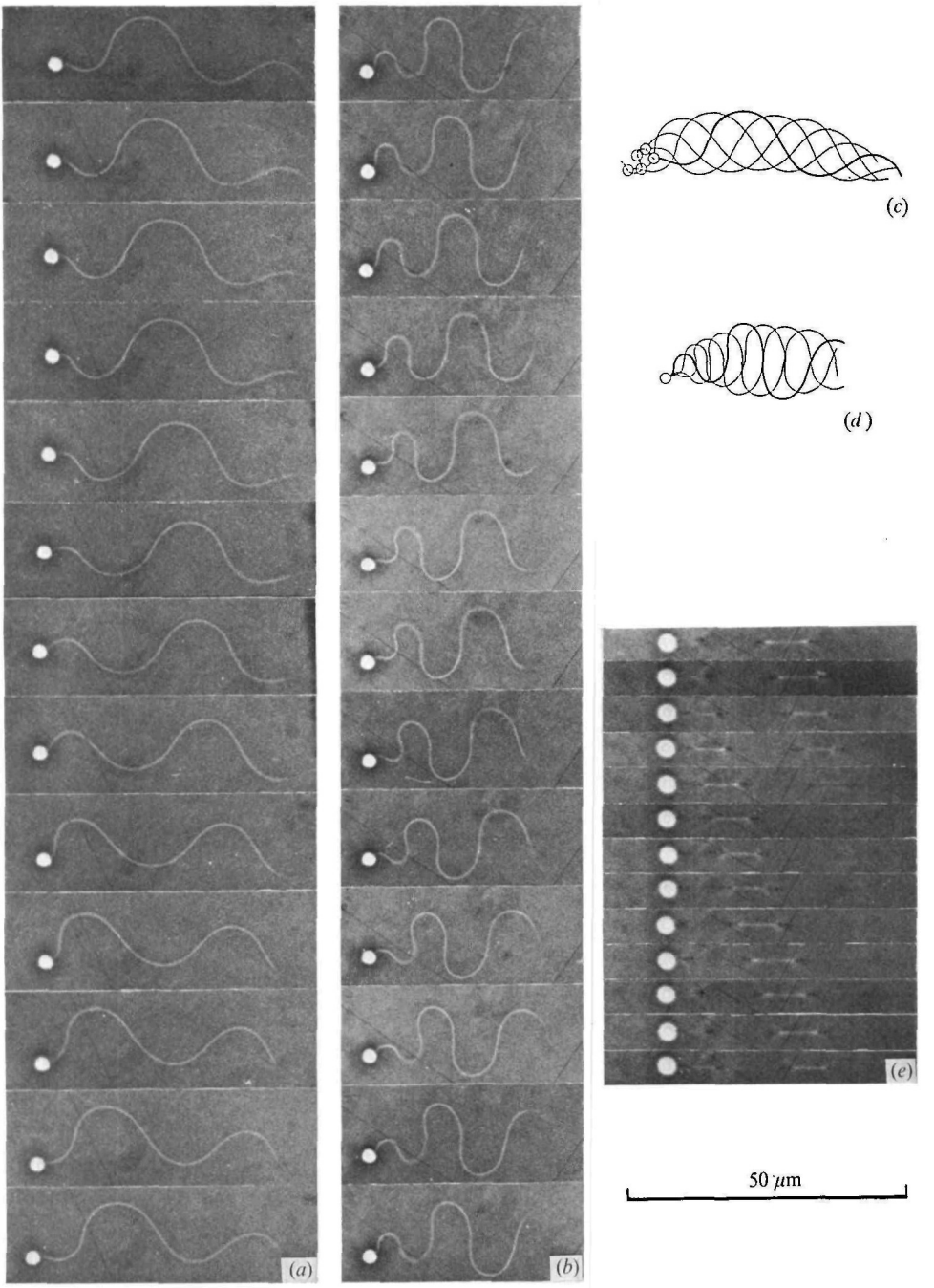

Fig. 1. Movement of the flagellum of starfish spermatozoa (*a* and *c*) swimming close to a coverslip and (*b*, *d* and *e*) adhering by the head to the cut edge of agar gel in sea water at 22 °C. The time interval between successive pictures from top to bottom is 2·1 ms in (*a*), 3·0 ms in (*b*) and 2·5 ms in (*e*). The beat plane is parallel to the plane of focus in (*a*) and (*b*), and is perpendicular to it in (*e*). In (*c*) and (*d*) the movement of spermatozoa is illustrated by superimposed waveforms, which are taken at one-quarter-cycle intervals from (*a*) and (*b*), respectively.

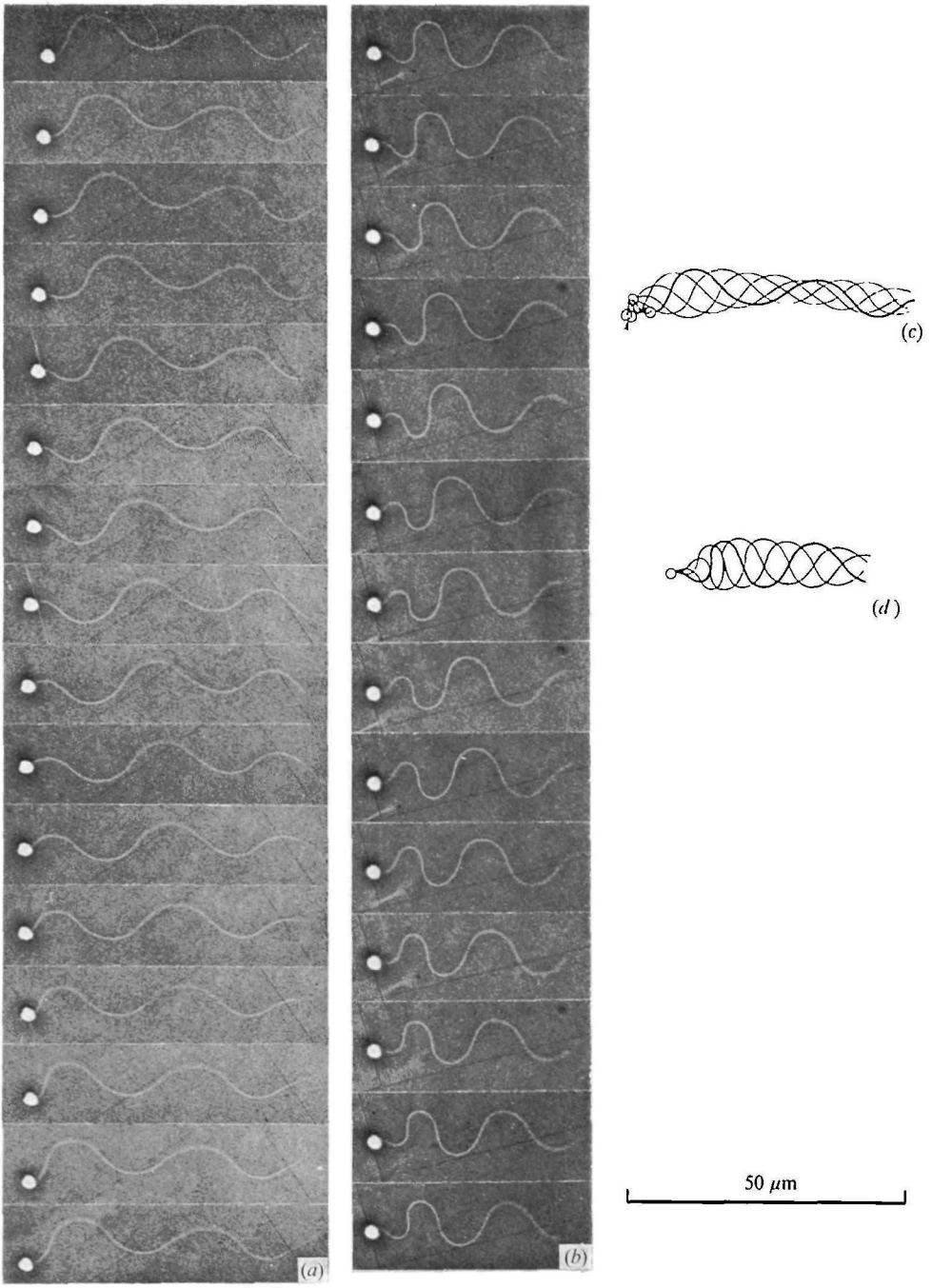

Fig. 2. Movement of the flagellum of starfish spermatozoa (*a* and *c*) swimming close to a coverslip and (*b* and *d*) adhering by the head to the cut edge of agar gel in sea water of increased viscosity (11 cP.) at 22 °C. The time interval is 24·8 ms in (*a*) and 18·8 ms in (*b*). (*c*) and (*d*) illustrate the movement of spermatozoa by superimposed waveforms, which are taken at one-quarter-cycle intervals from (*a*) and (*b*), respectively.

speeds of cells swimming close to the coverslip (Table 2). The beat plane of the flagellum seemed to be tangent to the screw surface of the spirals, because spermatozoa displayed the dashed-line image and hence the beat plane was known to be parallel to the optical axis when they crossed the spiral axis lying in the microscope field. Spiral swimming in this manner was interpreted by Gray (1955) to be a result of the combination of two rotations, one about the axis of propulsion (roll) and the other about that perpendicular to the beat plane (yaw); the third rotation (pitch) was not necessary for interpretation. If they were forced only to yaw, spermatozoa might swim in circular paths similar to spermatozoa swimming close to the coverslip. However, the radii of curvature of the spiral paths calculated, according to the geometry of the paths, to be $27{\cdot}3 \pm 1{\cdot}0$ μm (starfish) and $11{\cdot}2 \pm 2{\cdot}3$ μm (sea urchin) were significantly ($P < 0{\cdot}01$) smaller than those of circular paths of spermatozoa swimming close to the coverslip (cf. Table 2). The observation that the flagellar beat frequency, the speed of propulsion and the curvature of the path are different in swimming spermatozoa at different locations, close to or far from the coverslip surface, suggests that the presence of a solid surface mechanically affects the movement by modifying hydrodynamic loads during swimming.

The flagellum beat in a single stationary plane when adhering to agar gel (Figs. 1 *b*, *e* and 2 *b*), while in the case of egg jelly the spermatozoa stuck to it turned in such a way that the flagellar beat plane was tangent to a circular cone (this will be referred to as a boring motion). The beat frequency of starfish spermatozoa was lower when adhering to agar than when swimming freely (cf. Table 2).

Waveform

Before detailed theoretical analyses were made the waveforms of spermatozoa were reproduced by plotting $\mathbf{Q}(s, t)$. The standard deviation of $\mathbf{Q}(s, t)$ rarely exceeded $0{\cdot}1$ μm in repeated measurements, so the reproduction was believed to be sufficiently accurate for further analyses. Fig. 3 shows representative drawings of the waveforms of starfish spermatozoa (*a*) swimming about 300 μm from the coverslip, (*b*) swimming about 2 μm from it, and (*c*) adhering to agar.

Fig. 4 shows the variation of curvature $\gamma(s)$ with distance s of starfish spermatozoa (*a*) swimming about 300 μm from the coverslip, (*b* and *c*) swimming about 2 μm from it, and (*d* and *e*) adhering to agar. Differences in the flagellar waveform between cells distant from the coverslip (*a*) and close to it (*b*) are relatively small, indicating that the coverslip surface did not have a serious effect on the waveform. The waveforms of spermatozoa fixed by the head in agar (*d* and *e*) are considerably different from those of free-swimming spermatozoa (*a*, *b* and *c*) while differences in the waveform in media of different viscosities are small both for the free-swimming cells and for the fixed cells.

Fig. 5 shows the variation of the shaft angle $\phi^x(s, t)$ for starfish spermatozoa swimming close to the coverslip in sea water (*a*) and adhering to agar in sea water (*b*). In swimming sea-urchin spermatozoa, the peak value of ϕ^h with varying s (not shown), which corresponds to the angle that a 'straight region' (Brokaw, 1965) makes with the head axis, remained constant, as found by Goldstein (1975, 1976), within limited ranges of s (e.g. 8 μm $\sim$ 23 μm from the base leading to 'principal' bends (Gibbons, 1975) and 23 μm $\sim$ 42 μm leading to 'reverse' bends) as the wave

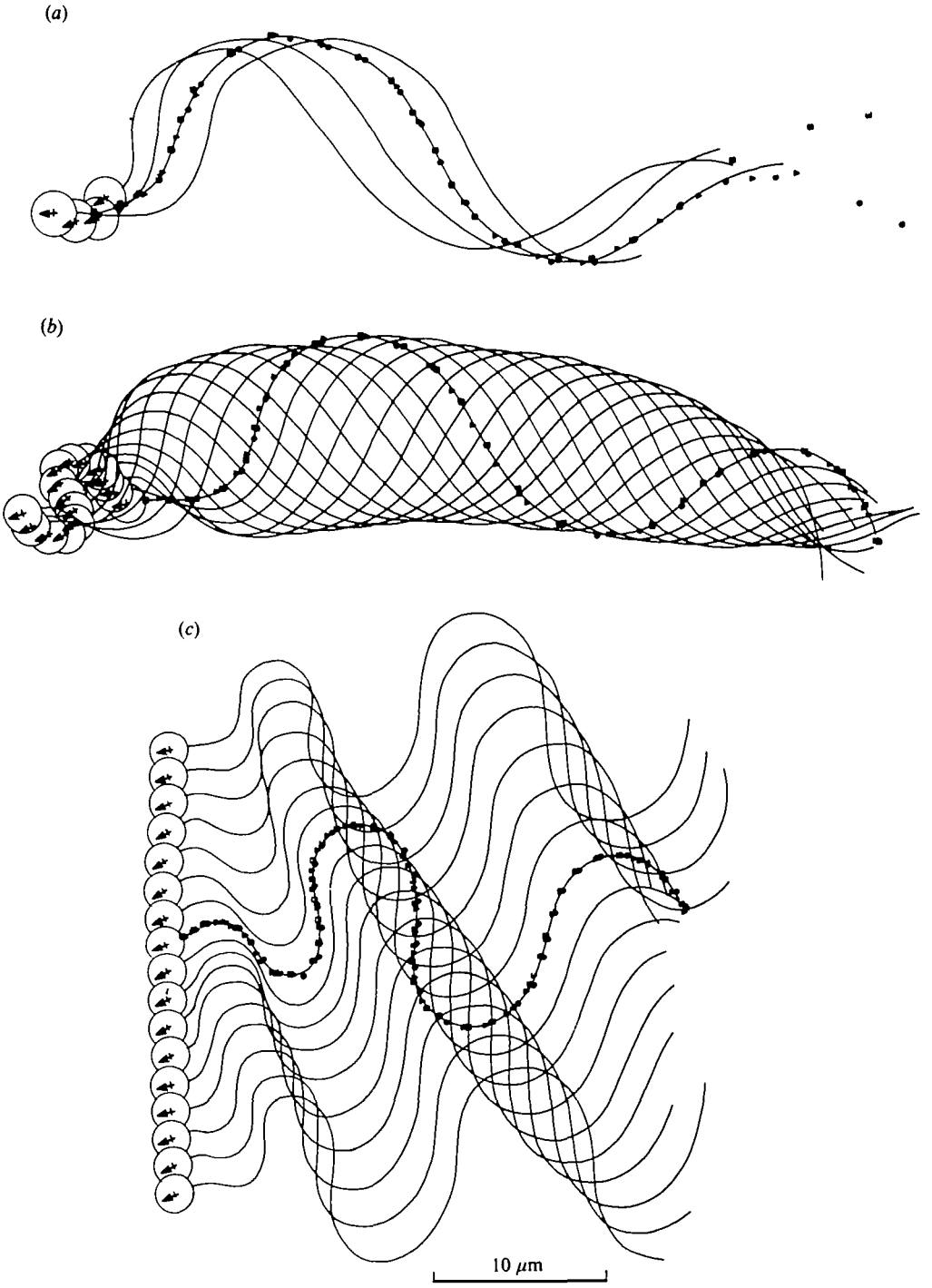

Fig. 3. Waveforms of the flagellum of starfish spermatozoa (*a*) swimming 300 μm below a coverslip, (*b*) swimming close to the coverslip and (*c*) adhering by the head to the cut edge of agar gel in sea water at 22 °C. The solid lines represent waveforms reproduced from the averaged $\mathbf{Q}(s, t)$ calculated from measurements on the coordinates of points on the flagellum; in each series of waveforms are indicated all points used in reproduction of one waveform by symbols □, ○ and ▷, and points for other waveforms are not shown here. Arrows in circles indicate the orientation of head. In (*c*) successive waveforms are displaced by 1·6 μm towards the bottom of the figure.

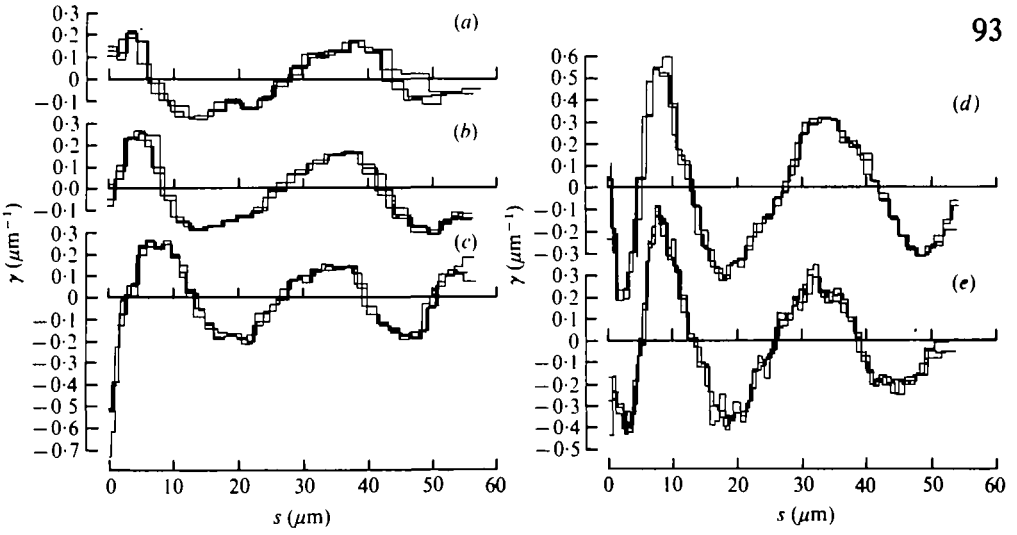

Fig. 4. Curvature $\gamma(s)$ of the flagellum of starfish spermatozoa (*a*) swimming 300 μm below a coverslip in sea water, (*b*) swimming close to a coverslip in sea water, (*c*) swimming close to a coverslip in sea water of increased viscosity (11 cP.), (*d*) adhering by the head to the cut edge of agar gel in sea water and (*e*) adhering by the head to the cut edge of agar gel in sea water of increased viscosity (11 cP.) at 22 °C. $\gamma(s)$ is expressed by three stepwise lines in all graphs; each line is obtained from a set of points recorded along the entire length of the flagellum. (See text for further details.)

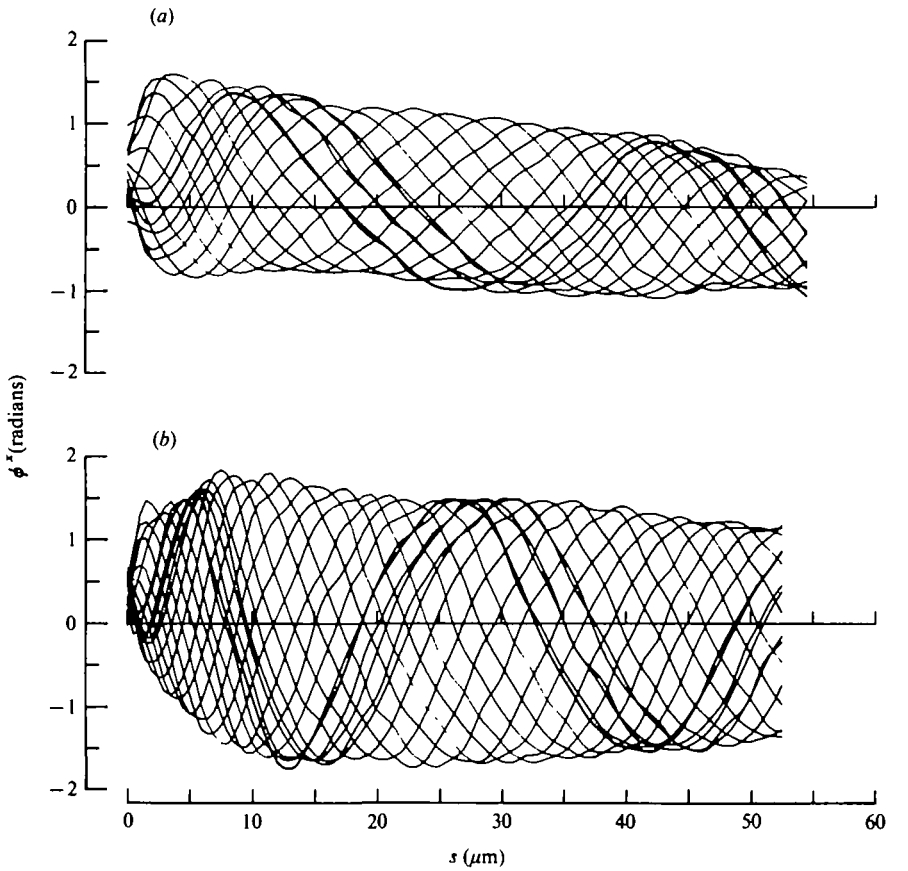

Fig. 5. Angular direction $\phi^x(s, t)$ of the flagellar shaft with respect to the X-axis (wave axis) of starfish spermatozoa (*a*) swimming close to a coverslip and (*b*) adhering by the head to the cut edge of agar gel. $\Delta s = 0{\cdot}5$ μm (see text).

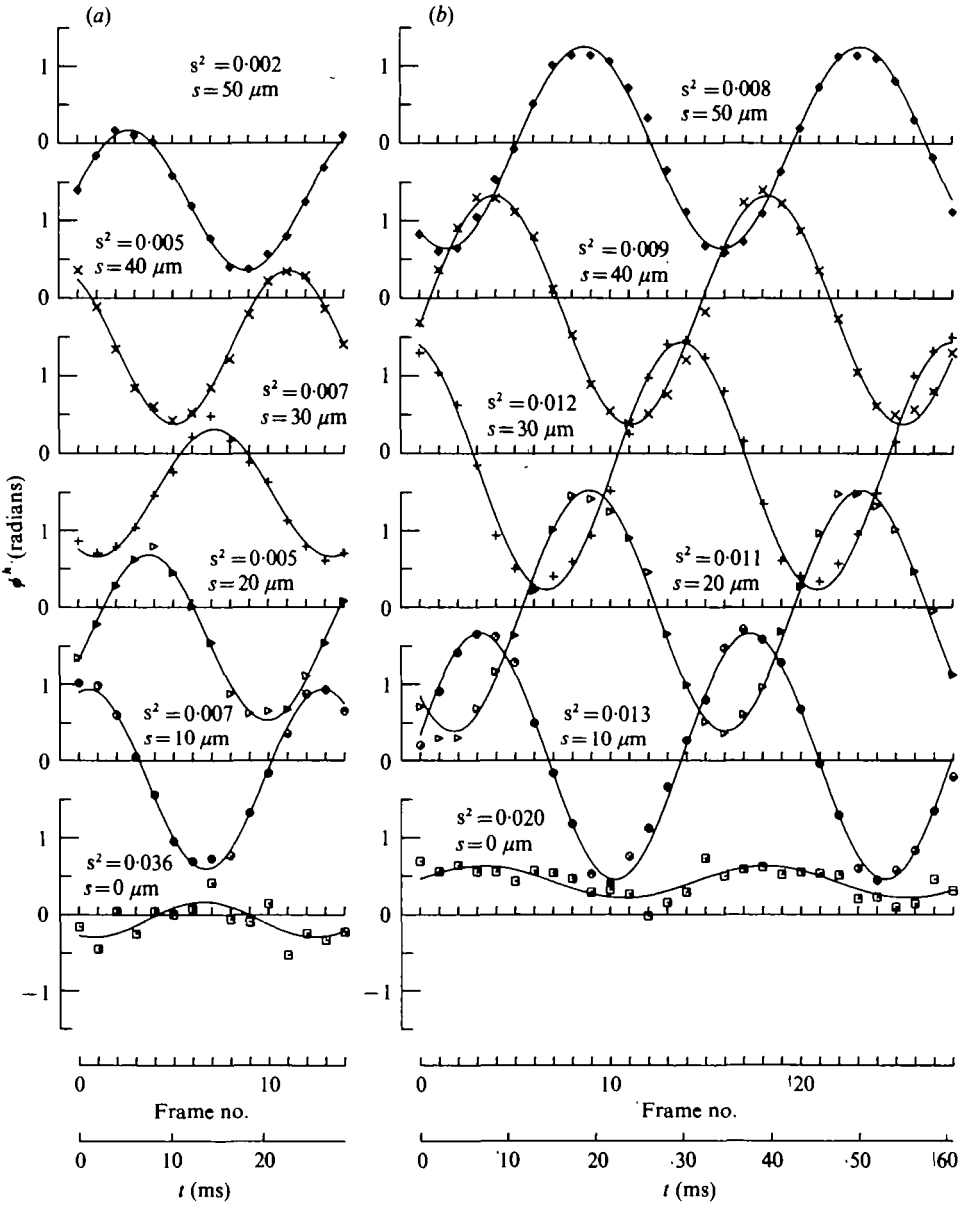

Fig. 6. Angular direction $\phi^h(s, t)$ of the flagellar shaft with respect to the axis of head of starfish spermatozoa (*a*) swimming close to a coverslip and (*b*) adhering by the head to the cut edge of agar gel. Symbols □, ○, ▷, +, × and ◇ represent observed data for s = 0, 10, 20, 30, 40 and 50 μm, respectively, and sine curves are least-squares fits to the observed data. s^2 is the variance of fit (see text).

propagates, though it was not always constant in starfish spermatozoa. Curves of ϕ against s appeared similar to sine waves within a short range of s, but both amplitude and wavelength change with distance s along flagellum.

It was found that the curves of ϕ were well fitted to simple sine curves when the shaft angle ϕ was plotted as a function of time for fixed s. To check the goodness

of fit, the applicability of equation (1) was tested using the method of least squares with varying t for various values of s at 0·5 μm intervals. Fig. 6 shows fitted sine curves and individual observed values of ϕ^h as functions of t at various points of 10 μm intervals along the starfish flagellum in a swimming spermatozoon (a) and an adhering one (b). Similar tests were also carried out on starfish spermatozoa in sea water of increased viscosity when swimming and when adhering, and sea-urchin spermatozoa swimming in sea water. The fit was always very good over the entire length of the flagellum examined. The variance s^2 of fit, which is a convenient measure of the goodness of fit (cf. Bevington, 1969), was usually 0·001 $\sim$ 0·01 rad^2. ϕ was replotted against s using equation (1) on the basis of this fitting and was found to compare favourably with that drawn directly from the original data. These results indicate that the directions of the flagellar shaft change sinusoidally with time at all parts along the flagellum, with the amplitude and the phase depending on distance s.

Fig. 7 shows the parameters $\phi_a(s)$, $S_\phi(s)$, $\omega(s)$ and $\phi_b(s)$ in equation (1), determined by the least-squares method. As shown in this figure, amplitude $\phi_a(s)$ first increases sharply and then changes slowly as distance s increases. It is noted that $\omega(s)$, representing 2π times the beat frequency, remains fairly constant along the entire length of the flagellum. $S_\phi(s)$ sharply increases in the range of about 10 μm from the base and increases at a constant rate as s increases. Since the conduction velocity of the wave is defined by $\omega(dS/ds)^{-1}$, it is concluded that the conduction velocity increases within about 10 μm from the base, approaching a constant value as the wave propagates. In the case of cells swimming in sea water (cf. Fig. 7*a*), $\phi_b(s)$, representing mean direction of the flagellum at s, changes almost linearly as s increases, though it is not always linear with s under other mechanical conditions (Fig. 7*b–d*). It should be noted that the asymmetry of waveforms (cf. Gibbons, 1975; Goldstein, 1977) is attributed to the variation of ϕ_b with s, and that $\partial\phi/\partial t$, which is directly proportional to the rate of sliding in the sliding microtubule model (see Discussion), is a pure sine function of time.

The curvature γ of the flagellar shaft can also be described by an equation similar to equation (1), that is,

$$\gamma(s, t) = \gamma_a(s) \cos \{S_\gamma(s) - \omega t\} + \gamma_b(s), \tag{11}$$

since γ is defined as $\partial\phi/\partial s$. Amplitude γ_a, phase angle S_γ and a constant representing mean curvature, γ_b, were determined, on the basis of the fitting of ϕ with equation (1), from the equations, $\gamma_a = \sqrt{(\alpha^2+\beta^2)}$, $S_\gamma = S_\phi + \pi/2 - \arctan(\alpha/\beta)$ and $\gamma_b = \partial\phi_b/\partial s$, where $\alpha = \partial\phi_a/\partial s$ and $\beta = \phi_a(\partial S_\phi/\partial s)$. As shown in Fig. 8, $\gamma(s, t)$ calculated directly from $\mathbf{Q}(s, t)$ and averaged in repeated measurements favourably agreed with the theoretical curve of equation (11). The amplitude of curvature, γ_a, vs. distance s for a starfish spermatozoon swimming in sea water is shown in Fig. 9(*a*) and that for a starfish spermatozoon adhering to agar is shown in Fig. 9(*b*). γ_a has a prominent peak at $s = 5 \sim 10$ μm, and changes rather slowly in the distal region of the flagellum. γ_b (not shown), which represents the degree of asymmetry of waveforms, is less than 10% of γ_a in these spermatozoa. In starfish spermatozoa γ_b was thus small relative to γ_a while in swimming sea-urchin spermatozoa γ_b was nearly 40% of γ_a at s exceeding 5 μm.

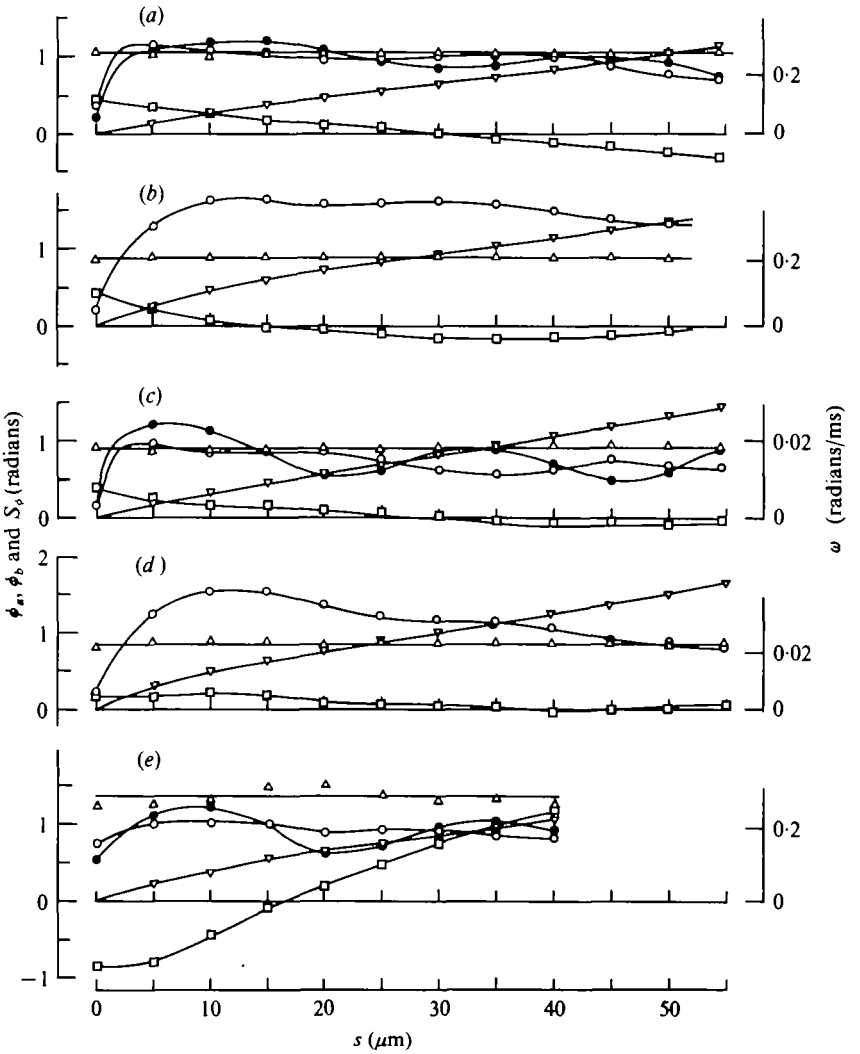

Fig. 7. Parameters ϕ_a^x(○), ϕ_a^h (●), S_ϕ^x (▽), ω (△) and ϕ_b^x (□) in equation (1) (see text) of starfish spermatozoa (*a*) swimming close to a coverslip in sea water, (*b*) adhering by the head to agar gel in sea water, (*c*) swimming close to a coverslip in sea water of increased viscosity (11 cP.), (*d*) adhering by the head to agar gel in sea water of increased viscosity (11 cP.), and (*e*) a sea-urchin spermatozoon swimming close to a coverslip in sea water at 22 °C. The parameters were determined by the method of least squares at intervals of 0·5 μm in s and are represented by continuous lines and the symbols given at intervals of 5 μm.

Bending moment due to external viscous resistance

Bending moment $m(s, t)$ due to the viscous resistance of the medium changed sinusoidally (cf. Brokaw, 1965). The moment about a point (s = 20 μm) on the flagellum is shown in Fig. 8 for a starfish spermatozoon swimming (*a*) and for one adhering (*b*), obtained from calculations using resistance coefficients C_H, C_N and C_L for model spermatozoa 2·0 μm from the coverslip surface (h = 2·0 μm in Table 1). It is noted that, in both cases, the change in the moment is preceded by the change in the curvature of the flagellum at the same point. In Fig. 9, amplitude of the curvature, γ_a, amplitude of the bending moment, m_a, and phase difference between the

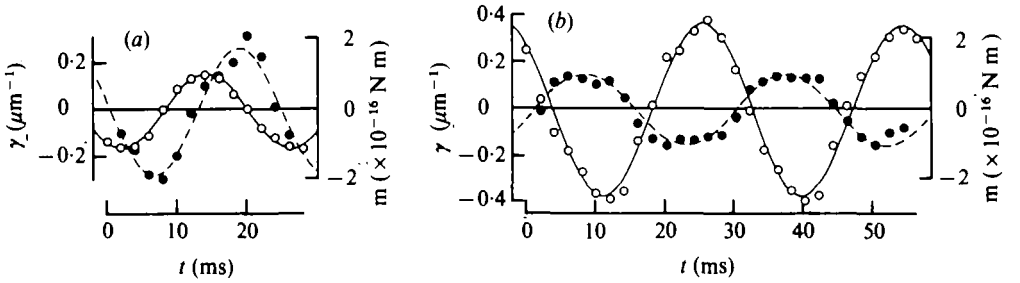

Fig. 8. Curvature $\gamma(s = 20\ \mu m, t)$ and bending moment $m(s = 20\ \mu m, t)$ of starfish spermatozoa (*a*) swimming close to a coverslip and (*b*) adhering by the head to the cut edge of agar gel in sea water at 22 °C. Solid sine curves are determined to match the observed data of the curvature (open circles), and dashed sine curves match the observed data of the bending moment (solid circles). The distance (h) of spermatozoa from the coverslip surface was assumed to be 2·0 μm in calculations of the bending moment.

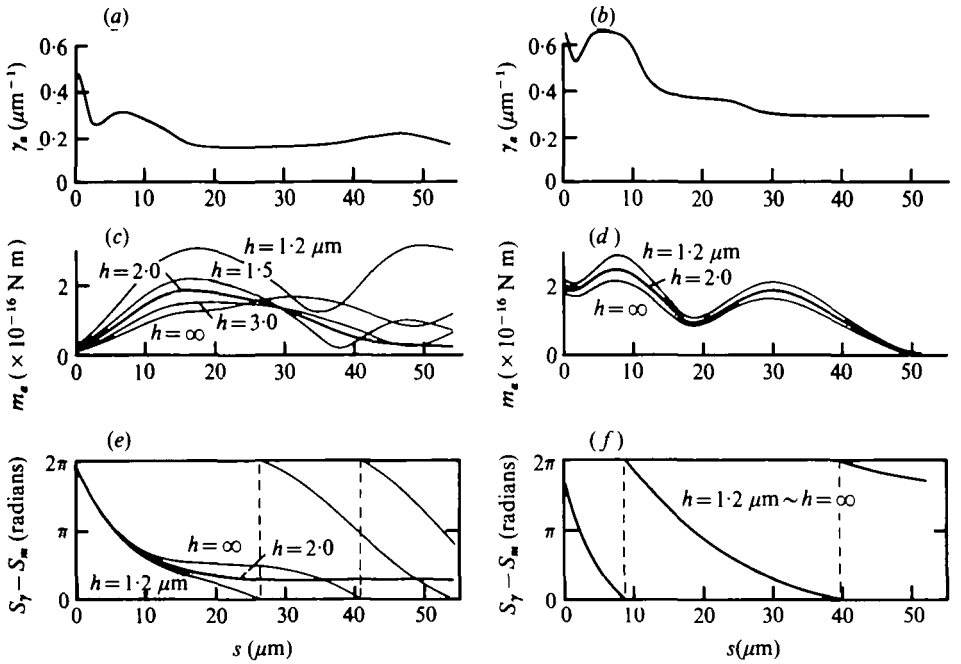

Fig. 9. The amplitude of curvature (γ_a, *a* and *b*) in equation (11), the amplitude of bending moment (m_a, *c* and *d*) in equation (10) and the phase difference ($S_\gamma - S_m$, *e* and *f*) between the curvature and the bending moment vs. the distance (s) from the base along the flagellum in the same spermatozoa swimming (*a*, *c* and *e*) and adhering (*b*, *d* and *f*) as shown in Fig. 8. Note that the amplitudes of the solid curves and those of the dashed curves shown in Fig. 8 and the phase differences between the solid and dashed curves are represented here as values at $s = 20\ \mu m$ in the corresponding graphs (thick curves). h is the distance of spermatozoa from the coverslip surface. (See text for further details.)

curvature and the moment, $S_\gamma - S_m$, are shown as functions of distance s for spermatozoa shown in Fig. 8; the moment was calculated for various values of h from 1·2 μm to ∞, because h could not be determined with exactitude. Although the moment calculated largely depends on h values in the case of the swimming spermatozoon (Fig. 9*c* and *e*), the result for $h = 2{\cdot}0\ \mu m$ is most realistic because m_a almost diminishes at the free terminal of the flagellum where the moment should be

zero. In the case of the adhering spermatozoon (Fig. 9*d*, *f*) calculations for various h values do not differ so much as in the case of the swimming spermatozoon.

As shown in this figure, no direct correlation was found in amplitude and in phase difference between the bending moment and the curvature with varying s either in the swimming or adhering spermatozoa (compare Fig. 9*a*, *b* with Fig. 9*c*, *d*, respectively). The observation indicates that the bending of the flagellum is not a result of passive deformation due to the viscous resistance of the medium. This will be discussed later.

DISCUSSION

Is the bending wave planar?

The fact that the bending wave was observed to be in focus over the entire length of the flagellum of spermatozoa indicates that the wave is substantially planar. However, if the bending wave were exactly planar, it would be difficult to explain the rotation of spermatozoa about the axis of propulsion (roll). The roll does not seem to need progression of cells, because spermatozoa adhering to egg jelly rotated without actual propulsion in boring motions. It is also unlikely that the roll of spermatozoa is induced by the rotation of the beat plane relative to the head, because the beat plane did not rotate when spermatozoa were adhering to agar gel. Therefore, the roll seems to be induced by some three-dimensional factors inherent in the flagellar movement.

It is possible to explain the roll of spermatozoa by assuming the existence of a minor component perpendicular to the major beat plane of the flagellar movement. The torque due to the viscous resistance acting on the head of swimming starfish spermatozoa is estimated to be 6×10^{-19} N m by the equation,

$$T = 16\pi^2\eta n a^3, \tag{12}$$

where η is the viscosity of the medium, n is the frequency of the roll and a is the radius of the head. The corresponding torque for swimming sea-urchin spermatozoa was found to be 9×10^{-19} N m, by using an equation for the torque acting on a prolate spheroid rotating about its polar axis (cf. Jeffrey, 1915). By calculating the torque for helical waves (cf. Coakley & Holwill, 1972), it was found that a torque of the order of 10^{-18} N m can be generated if there is a component of 0·2 μm amplitude perpendicular to the major beat plane of the flagellum (5 μm major amplitude and 45 Hz frequency). By ordinary microscopic observation such a minor component would hardly be recognized and the movement would appear to be almost planar.

It has been noticed that the direction of propulsion is usually anticlockwise in spermatozoa moving in circles on the upper surface of slide glass and opposite when on the lower surface of coverglass (cf. Holwill, 1966). Gray (1955) interpreted this observation by assuming that spermatozoa travel in the manner of left-handed screws when swimming freely and that they are trapped by the surface that they reach. He also pointed out that spermatozoa should roll in the anticlockwise direction around the axis of propulsion, regardless of the direction of yawing, if they travelled in left-handed spirals and kept the beat plane in contact with the screw surface. The above facts and Gray's explanation are well in accordance with the observation in the present

study of starfish and sea-urchin spermatozoa. The sense of the three-dimensional flagellar movement (flattened helical wave), which explains the roll of spermatozoa, should be right-handed to account for the left-handed spiral swimming of spermatozoa.

Reliability of bending moment calculations

The results of calculations of the bending moment acting on the flagellum due to the viscous resistance of the medium depend on the applicability of Gray & Hancock's (1955) local resistance coefficient theory to the present problem, the choice of the values of the resistance coefficients and the accuracy in recordings of the actual waveform of the flagellum. Gray & Hancock's (1955) theory appears to be reliable in calculations of resistance and moment, if appropriate values for the resistance coefficients are used, though the evaluation of the theory is beyond the extent of discussion in the present study (cf. Lighthill, 1976).

In the case of the swimming spermatozoa the bending moment was calculated by integrating moments, given by equations (8) and (9), due to the local resistances acting on the proximal part of the spermatozoon to the point in question, while in the adhering spermatozoon it was calculated using the resistances on the distal part. Theoretically, the bending moment calculated from the resistances of the proximal part must be equal to that from the resistances on the distal part, but there were some discrepancies between them; for example, the bending moment at $s = 20\,\mu$m for a swimming spermatozoon calculated from proximal resistances (shown in Fig. 8*a*) was smaller by 38% in amplitude than that calculated from distal resistances (not shown) and preceded by 1·1 radian in phase. The bending moment calculated from distal resistances seemed to be less reliable than that from proximal resistances, since the thin terminal piece of the flagellum (end piece, cf. Afzelius, 1955, 1959; Brokaw, 1965; about 7 μm long in starfish spermatozoa) recorded rather inaccurately or missed in recordings must be taken into account.

Evidence for active bending wave

Baba & Hiramoto (1970*b*) found in cilia of *Mytilus* that the major increase and decrease in the curvature of the shaft preceded those of the bending moment due to the viscous resistance of the medium. This observation verified the conclusion, obtained by Machin (1958) from his theoretical calculations in flagella, that the bending wave is generated by active internal forces rather than external ones applied to the flagellum, because the bending moment would change in parallel with or precede the change of the curvature, if the bending wave were passive in nature. The same conclusion was obtained by the analysis of flagellar movement in starfish spermatozoa in the present study. Furthermore, the present observation that the variation of the curvature is not directly correlated with the bending moment both in amplitude and in phase confirms the above conclusion.

Sine-generated bending wave

Gray (1955) obtained the first photographic recordings of the waveform of the sea-urchin sperm flagellum. He described the waveform as a sine wave and used it to explain the propulsion of the sperm in hydrodynamic terms. After a decade, Brokaw

(1965) recorded the waveform in some invertebrate spermatozoa by an improved technique, and reported that the waveform could be well matched by circular arcs connected by straight lines (arc-line curve) rather than sine waves. However, it was found by careful measurement in the present study that the waveforms of beating flagella are matched neither by sine curves as shown in Fig. 3, nor by Brokaw's arc-line curves as shown in Fig. 4, in which curvature changes along the flagellum in a continuous fashion rather than a stepwise fashion (from zero to a steady value expected from arc-line curves).

It has been pointed out by several investigators (Brokaw, Goldstein & Miller, 1970; Brokaw, 1972; Rikmenspoel, 1971; Silvester & Holwill, 1972) that the waveforms of flagella, especially those of a large amplitude, appear similar in shape to the meander of a river. By using sine-generated curves which approximate well meander curves (Langbein & Leopold, 1966; Leopold & Langbein, 1966), Sarashina (1974) obtained a good approximation to the waveform that Brokaw (1965) photographed and described to be an arc-line curve. Direct measurement of flagellar movement in the present study has clearly shown that the angular direction at any point along the flagellum changes as a sine function of time in all cases examined: spermatozoa in normal sea water and sea water of increased viscosity when swimming and when adhering to agar. It seems to be one of the fundamental natures of the flagellar movement that the angular direction changes in a sinusoidal fashion, because this nature is always kept while the parameters of the sine function vary with a variety of mechanical conditions. Since equation (1) is a good approximation to the bending wave, the curvature γ ($= \partial\phi/\partial s$) of the flagellum should also be a sine function of time, which was confirmed by observation.

It has been observed by previous investigators (e.g. Kaneda, 1965; Brokaw, 1966, 1974; Brokaw & Gibbons, 1975; Okuno & Hiramoto, 1976) and is confirmed in the present study that various mechanical conditions (e.g. whether the head is free or fixed, and increased viscosity of the medium) may significantly change the flagellar waveform and the beat frequency. This suggests that the external loads can influence the internal regulatory mechanism of the flagellum. In order to elucidate this internal regulatory mechanism, various hypotheses have been proposed (Lubliner & Blum, 1977; Rikmenspoel, 1971; Brokaw, 1976*a*, *b*; Brokaw & Gibbons, 1975 and further references therein), and their legitimacy was examined by comparing the conclusion derived from hypotheses with experimental data of flagellar movement obtained under various conditions. The quantitative results including parameters of the wave equation in the present experiment (cf. Fig. 7) may provide useful data for theoretical works in this field.

It has been observed that the microtubules in the axoneme slide during flagellar movement while the length of the microtubules remains constant (cf. Satir, 1974). In this case, the amount of sliding (u) between outer doublet microtubules would be directly proportional to the angle ϕ^o formed by the axis of the axoneme and the tangent to the basal region (where no sliding occurs). Because the basal region is believed to be fixed in direction to the head, equation (1) is applicable to ϕ^o as well as ϕ^h; suffix o will be omitted in the following discussion when it is not necessary to refer to the reference line of the shaft angle.

Silvester & Holwill (1972) calculated the energy stored in or required to deform

hypothetical elastic elements in flagella, and showed that the total elastic energy, which is proportional to $\int_0^{\Lambda} (\partial\phi/\partial s)^2\, ds$ in one wavelength Λ measured along the flagellum, is smallest in the case of a meander (which is virtually a sine-generated wave) among the cases of three proposed waveforms (sine wave, meander, and arc-line wave) with the same wavelength and the same propulsion velocity. In the sliding microtubule model, the rate of energy expenditure due to internal friction by sliding would be proportional to the square of the rate of sliding, $(\partial u/\partial t)^2$, and consequently to $(\partial\phi^0/\partial t)^2$. The frictional energy expenditure for one beat cycle τ is, therefore, proportional to $\int_0^{\tau} (\partial\phi^0/\partial t)^2\, dt$, which is equivalent to $\int_0^{\Lambda} (\partial\phi/\partial s)^2\, ds$ if the wave had a constant amplitude and wavelength along the flagellum. Therefore, in the case of sine-generated waves, both the elastic potential energy and the frictional energy expenditure become minimal for a given propulsion velocity. This conclusion suggests that the flagellar movement is regulated to give an optimum condition for the system.

In the sliding microtubule model, active sliding force has to be equal to the internal resistance due to the deformation of the axoneme and the resistance exerted by the medium. The internal resistance includes the elastic and frictional resistances set up by the sliding (shear) and the elastic resistance due to the bending of the microtubules; these resistances would be proportional to ϕ^0, $\partial\phi^0/\partial t$ and $\partial\phi/\partial s$ $(= \gamma)$, respectively. Since ϕ^0, $\partial\phi^0/\partial t$ and $\partial\phi/\partial s$ could be expressed by sine functions of time of the same ω (angular velocity) plus different constants, the total internal resistance would change as sine functions of time of the same ω. Since bending moment m due to the external resistance of the medium was observed to change sinusoidally with the same ω as shown in Fig. 8 (cf. Brokaw, 1965), the resistance for sliding $(= \partial m/\partial s)$ due to the external resistance would also change sinusoidally with time. Therefore, it seems likely that the sliding force is generated as a sine function of time.

From observations of microtubule sliding in trypsin-digested axonemes (Summers & Gibbons, 1971, 1973) and of cross-bridging of microtubules in rigor flagella (Gibbons & Gibbons, 1974), Gibbons (1975) suggested that almost all peripheral tubules would participate in force generation and would always slide in one direction with respect to their adjacent tubules (unipolar sliding hypothesis), and Sale & Satir (1977) and Satir & Sale (1977) determined the sense of polarity of sliding by electron microscopy. The unipolar sliding between microtubules would require well-regulated activation of force-generation in the axoneme. Attempts have been made to explain flagellar movement by regulated activation of the contractile machinery in the axoneme by several authors (e.g. Gray, 1955; Bradfield, 1955; Párducz, 1967; Rikmenspoel, 1971; Costello, 1973; Machemer, 1977; Sale & Satir, 1977; Brokaw, 1977).

The authors propose a model for flagellar movement as follows. In this model, it is assumed that the site at which sliding force is generated changes from one tubule couple to the neighbouring one around the nine peripheral doublet microtubules and at the same time in the longitudinal direction of the microtubules, so that the active site propagates around the axoneme forming a helical path. To explain the three-dimensional movement of flagella, similar models were proposed by Rikmenspoel (1971) and Machemer (1977) on the basis of sliding model and by Bradfield (1955), Gray (1955), Párducz (1967), and Costello (1973) assuming helical propagation of

contractile activity or bending of microtubules. The site of tubule interaction should propagate towards the tip along the axoneme and anticlockwise around it (viewed from base) to account for the left-handed spiral swimming observed in sperm, and clockwise for ciliary movement in *Paramecium* (Machemer, 1977). For the planar movement of flagella, it is assumed that only the component in the beating plane of the couple of forces by tubule interaction is effective by a special (presumably, structural) mechanism in the flagellum. The observations that the principal bending plane is almost perpendicular to the central pair of singlet tubules and the presence of bridging between No. 5 and No. 6 doublet microtubules (Afzelius, 1959; cf. Summers, 1975) suggest existence of this mechanism. In the present model, it is possible for the flagellum to generate the active motive force in a sinusoidal fashion in the principal bending plane, even when the motive force generated by tubule interaction at each site does not change sinusoidally, because the effective component to the bending plane of the sliding couple by any tubule interaction is the couple multiplied by the sine of the angle made by the vector couple and the plane, and therefore the effective sliding couple in this plane change practically in a sinusoidal fashion as the site of interaction propagates at a constant speed around the axoneme. The present model is compatible with the unipolar sliding model mentioned above.

In the present study the authors described bending waves in some echinoderm sperm flagella using a simple equation of the same form. Further experimental works will be done for analysis of parameters in the equation under various experimental conditions. The automatic tracking system of the photographic images, which was recently achieved by Silvester & Johnston (1976), will be useful for such an analysis.

We are very grateful to Professors H. Kinosita and K. Takahashi for interest, encouragement, criticism and patience. This work was supported by Research Expenditures of the Ministtry of Education, Science and Culture given to us from 1969 through 1977 and a Mainichi Science Encouragement Award in 1972. We thank Dr M. E. J. Holwill for critical reading of the draft. Thanks are also due to the Director and the staff of Misaki Marine Biological Station of the University of Tokyo for providing materials and facilities, and Professors F. Kanno and K. Ishii of Hosei University, and Professor H. Sugi of Teikyo University for their suggestions to use film analysers.

REFERENCES

AFZELIUS, B. A. (1955). The fine structure of the sea urchin spermatozoa as revealed by the electron microscope. *Z. Zellforsch. mikrosk. Anat.* **42**, 134–148.

AFZELIUS, B. A. (1959). Electron microscopy of the sperm tail. *J. Biophys. Biochem. Cytol.* **5**, 269–278.

BABA, S. A. & HIRAMOTO, Y. (1970*a*). High-speed microcinematography of ciliary movement. *Zool. Mag., Tokyo* **79**, 8–13.

BABA, S. A. & HIRAMOTO, Y. (1970*b*). A quantitative analysis of ciliary movement by means of high-speed microcinematography. *J. exp. Biol.* **52**, 675–690.

BEVINGTON, P. R. (1969). *Data Reduction and Error Analysis for the Physical Sciences.* New York: McGraw Hill.

BRADFIELD, J. R. G. (1955). Fibre patterns in animal flagella and cilia. *Symp. Soc. Exp. Biol.* **9**, 306–332.

BROKAW, C. J. (1965). Non-sinusoidal bending waves of sperm flagella. *J. exp. Biol.* **43**, 155–169.

BROKAW, C. J. (1966). Effects of increased viscosity on the movements of some invertebrate spermatozoa. *J. exp. Biol.* **45**, 113–139.

BROKAW, C. J. (1972). Flagellar movement: A sliding filament model. *Science* **178**, 455–462.

BROKAW, C. J. (1974). Movement of the flagellum of some marine invertebrate spermatozoa. In *Cilia and Flagella* (ed. M. A. Sleigh), pp. 93–109. London and New York: Academic Press.

BROKAW, C. J. (1976*a*). Computer simulation of movement-generating cross-bridges. *Biophys. J.* **16**, 1013–1027.

BROKAW, C. J. (1976*b*). Computer simulation of flagellar movement. IV. Properties of an oscillatory two-stage cross-bridge model. *Biophys. J.* **16**, 1029–1041.

BROKAW, C. J. (1977). Is the 9+2 pattern of flagellar and ciliary axonemes an efficient arrangement for generating planar bending? *J. Mechanochem. Cell Mot.* **4**, 101–111.

BROKAW, C. J. & GIBBONS, I. R. (1975). Mechanisms of movement in flagella and cilia. In *Swimming and Flying in Nature, vol. I* (ed. T. Y.-T. Wu, C. J. Brokaw and C. Brennen), pp. 89–126. London and New York: Plenum Press.

BROKAW, C. J., GOLDSTEIN, S. F. & MILLER, R. L. (1970). Recent studies on the motility of spermatozoa from some marine invertebrates. In *Comparative Spermatology* (ed. B. Baccetti), pp. 475–497. London and New York: Academic Press.

COAKLEY, C. J. & HOLWILL, M. E. J. (1972). Propulsion of micro-organisms by three-dimensional flagellar waves. *J. theor. Biol.* **35**, 525–542.

COSTELLO, D. P. (1973). A new theory on the mechanics of ciliary and flagellar motility. II. Theoretical considerations. *Biol. Bull.* **145**, 292–309.

FUJII, T., UTIDA, S. & MIZUNO, T. (1955). Reaction of starfish spermatozoa to histidine and certain other substances considered in relation to zinc. *Nature, Lond.* **176**, 1068–1069.

GIBBONS, I. R. (1975). The molecular basis of flagellar motility in sea urchin spermatozoa. In *Molecules and Cell Movement* (ed. S. Inoué and R. Stephens), pp. 207–231. New York: Raven Press.

GIBBONS, I. R. & GIBBONS, B. H. (1974). The fine structure of rigor wave axonemes from sea-urchin sperm flagella. *J. Cell Biol.* **63**, 110*a*.

GOLDSTEIN, S. F. (1975). Morphology of developing bends in sperm flagella. In *Swimming and Flying in Nature* (ed. T. Y. Wu, C. J. Brokaw and C. Brennan), pp. 127–132. New York: Plenum Press.

GOLDSTEIN, S. F. (1976). Form of developing bends in reactivated sperm flagella. *J. exp. Biol.* **64**, 173–184.

GOLDSTEIN, S. F. (1977). Asymmetric waveforms in echinoderm sperm flagella. *J. exp. Biol.* **71**, 157–170.

GRAY, J. (1955). The movement of sea-urchin spermatozoa. *J. exp. Biol.* **32**, 775–801.

GRAY, J. & HANCOCK, G. J. (1955). The propulsion of sea-urchin spermatozoa. *J. exp. Biol.* **32**, 802–814.

HAPPEL, J. & BRENNER, H. (1965). *Low Reynolds Number Hydrodynamics*. Englewood Cliffs: Prentice Hall.

HOLWILL, M. E. J. (1966). Physical aspects of flagellar movement. *Physiol. Rev.* **46**, 696–785.

JEFFERY, G. B. (1915). On the steady rotation of a solid of revolution in a viscous fluid. *Proc. London Math. Soc.* **14**, 327–338.

KANEDA, Y. (1965). Movement of sperm tail of frog. *J. Fac. Sci. Univ. Tokyo*, sec. IV, **10** (P3), 427–440.

KATZ, D. F. & BLAKE, J. R. (1975). Flagellar motions near walls. In *Swimming and Flying in Nature, Vol. I* (ed. T. Y.-T. Wu, C. J. Brokaw and C. Brennen), pp. 173–184. London and New York: Plenum Press.

LANGBEIN, W. B. & LEOPOLD, L. B. (1966). River meanders – Theory of minimum variance. *U.S. Geol. Survey Prof. Paper* **422**–H, 1–15.

LEOPOLD, L. B. & LANGBEIN, W. B. (1966). River meanders. *Sci. Am.* **214**, 60–70.

LIGHTHILL, J. (1976). Flagellar hydrodynamics. *Siam Rev.* **18**, 161–230.

LUBLINER, J. & BLUM, J. J. (1977). Analysis of bend initiation in cilia according to a sliding filament model. *J. theor. Biol.* **69**, 87–99.

MACHEMER, H. (1977). Motor activity and bioelectric control of cilia. *Fortschr. Zool.* **24**, 195–210.

MACHIN, K. E. (1958). Wave propagation along flagella. *J. exp. Biol.* **35**, 796–806.

OKUNO, M. & HIRAMOTO, Y. (1976). Mechanical stimulation of starfish sperm flagella. *J. exp. Biol.* **65**, 401–413.

PÁRDUCZ, B. (1967). Ciliary movement and coordination in ciliates. *Int. Rev. Cytol.* **21**, 91–128.

POWELL, M. J. D. (1965). A method for minimizing a sum of squares of non-linear functions without calculating derivatives. *Computer J.* **7**, 303–307.

RIKMENSPOEL, R. (1971). Contractile mechaniams in flagella. *Biophys. J.* **11**, 446–463.

SALE, W. S. & SATIR, P. (1977). The direction of active sliding of microtubules in *Tetrahymena* cilia. *Proc. natn. Acad. Sci. U.S.A.* **74**, 2045–2049.

SARASHINA, T. (1974). Numerical analysis on wavy track of nematodes. *Rep. Hokkaido Prefect. Agric. Exp. Stn.* **23**, 1–48.

SATIR, P. (1974). The present status of the sliding microtubule model of ciliary motion. In *Cilia and Flagella* (ed. M. A. Sleigh), pp. 131–142. London and New York: Academic Press.

SATIR, P. & SALE, W. S. (1977). Tails of *Tetrahymena*. *J. Protozool.* **24**, 498–501.

SILVESTER, N. R. & HOLWILL, M. E. J. (1972). An analysis of hypothetical flagellar waveforms. *J. theor. Biol.* **35**, 505–523.

SILVESTER, N. R. & JOHNSTON, D. (1976). An electro-optical curve follower with analogue control. *J. Phys. E. Sci. Instr.* **9**, 990–995.

SUMMERS, K. (1975). The role of flagellar structures in motility. *Biochim. Biophys. Acta* **416**, 153–168.

SUMMERS, K. & GIBBONS, I. R. (1971). Adenosine Triphosphate-induced sliding of tubules in trypsin-treated flagella of sea-urchin sperm. *Proc. natn. Acad. Sci. U.S.A.* **68**, 3092–3096.

SUMMERS, K. & GIBBONS, I. R. (1973). Effects of trypsin digestion on flagellar structures and their relationship to motility. *J. Cell Biol.* **58**, 618–629.

TAKAISHI, Y. (1958). The forces on a long straight circular cylinder moving in a semi-infinite viscous liquid bounded by a plane wall. *Mem. Ehime Univ.*, Sec. II **3**, 29–35.